



Numerical Heat Transfer, Part A: Applications

An International Journal of Computation and Methodology

ISSN: 1040-7782 (Print) 1521-0634 (Online) Journal homepage: <http://www.tandfonline.com/loi/unht20>

Comprehensive review and study of the buoyant air flow within positive-pressure hospital operating rooms

J. P. Abraham, B. D. Plourde & L. J. Vallez

To cite this article: J. P. Abraham, B. D. Plourde & L. J. Vallez (2017) Comprehensive review and study of the buoyant air flow within positive-pressure hospital operating rooms, Numerical Heat Transfer, Part A: Applications, 72:1, 1-20, DOI: [10.1080/10407782.2017.1353368](https://doi.org/10.1080/10407782.2017.1353368)

To link to this article: <http://dx.doi.org/10.1080/10407782.2017.1353368>



Published online: 08 Aug 2017.



Submit your article to this journal [↗](#)



Article views: 39



View related articles [↗](#)



View Crossmark data [↗](#)

Full Terms & Conditions of access and use can be found at
<http://www.tandfonline.com/action/journalInformation?journalCode=unht20>



Comprehensive review and study of the buoyant air flow within positive-pressure hospital operating rooms

J. P. Abraham, B. D. Plourde, and L. J. Vallez

School of Engineering, University of St. Thomas, St. Paul, Minnesota, USA

ABSTRACT

A comprehensive investigation is provided on the flow of air within a positive-pressure operating room during a simulated surgery. The simulated surgery made use of an over-body patient-warming blanket whose purpose is to maintain patient temperatures. One issue to be studied was whether a forced-air patient-warming unit with the blanket caused airflow disturbances at the surgical site that would otherwise not occur without the blanket. In the study, measurements from an operating room, including dimensions, flowrates, temperatures, and the positions of potential flow blockages were taken. Airflow simulated using the large-eddy simulation method showed that at no time, and under no conditions did the device cause potentially unclean air to intrude into the sterile surgical field during the operation of the warming device. In addition, a series of flow-visualization experiments made with neutrally buoyant tracers showed the surgical site was washed by ultraclean air from the ventilation system of the operating room regardless of whether the patient-warming device was being used. A comparison of the numerical simulations and experiments showed a near perfect match in temperature measurements and flow patterns. The mutually reinforcing simulations and experiments lend added credibility to the results.

ARTICLE HISTORY

Received 24 April 2017

Accepted 16 June 2017

1. Introduction

Maintenance of normothermia during surgery, particularly when general anesthesia is used, is important for patient outcomes. Adequate accounting for heat transfer processes to and from the patient is complicated by the interrelated actions between systems that warm the patient, the patient's body, and the surrounding environment. Many studies have investigated both local and global biologic heat transfer situations [1–20] and many of these studies have accounted for physiologic processes such as blood perfusion, respiration, flow through porous media, and other factors [21–32]. In addition, recent studies have taken advantage of many advancements in numerical simulation algorithms, computational hardware, and experimental methods articulated in Refs [33–48].

Convective warming systems typically involve impingement of heated air, through a perforated blanket, onto a patient's body during surgery. A recent review of this technology was provided in Ref [49]. Readers are directed to that reference for more detail regarding heat transfer calculations within the patient body. However, it is noted here that the literature is somewhat developed in this regard and includes multiple whole-body thermal models [50–55] and in some cases, the studies incorporate thermoregulatory responses of the organism [56–70].

Multiple studies have given consideration to how inhibitions of the normal human thermoregulatory system can contribute to problems during surgery [71–78]. Collectively, these studies report that

CONTACT J. P. Abraham ✉ jpabraham@stthomas.edu ☎ School of Engineering, University of St. Thomas, 2115 Summit Ave., St. Paul, MN 55105-1079, USA.

Color versions of one or more of the figures in the article can be found online at www.tandfonline.com/unht.

© 2017 Taylor & Francis

| Nomenclature | | | |
|--------------|-------------------------------------|----------------------|---------------------|
| C_o | courant number | <i>Greek symbols</i> | |
| p | pressure | γ | filtering function |
| t | time | ρ | density |
| u_i | velocity in tensor form | τ | shear stress |
| x_i | coordinate direction in tensor form | ν | kinematic viscosity |
| | | φ | filtering variable |

during surgery, particularly when anesthesia is used, shivering and vasoconstriction occur at lower temperatures. Consequently, it is a goal of patient-warming systems to help avoid lowered core temperatures throughout the surgical and recovery periods.

One common patient-warming system is the forced-air convection type. As stated earlier, these devices work by impinging heated air against the skin of the patient. The systems that accomplish this are typically air-inflated blankets that are connected to a blower-heating system. Ambient air is drawn into the blower casing, heated to approximately 43°C, and then passed into the blanket by means of a flexible tube. The inflated blanket is permeable with a multitude of small holes that direct air toward the patient.

In some manifestations, these blankets lie atop the patient (over-body blankets) while in other scenarios, they are underneath the patient (under-body blankets). Some blankets cover nearly the entire patient body (full-body blankets), whereas others heat only the upper- or lower-body portions (upper-body or lower-body blankets). Questions have been raised about whether spent air from the blankets may alter the normal airflow within the operating room. It is this issue which is the focus of the current study.

Prior to exhibiting the study methodology, the relevant literature on this issue of potential flow disturbances will be discussed. Numerous studies have been carried out on this issue, mainly confined to medical-journal venues [79–105]. Generally, the evidence supports the conclusion that forced-air warming blankets are safe and effective; however, a small minority of studies has cast doubt on that conclusion and it is recognized that within the medical community there may still be questions about the potential for an operating room ventilation flow to be disturbed by a forced-convection system. To the best knowledge of the authors, there is no comprehensive simulation that fully accounts for the complex flow phenomena such as unsteady vortex shedding, buoyancy, and various scales of turbulence. Such a comprehensive numerical study will be performed here and comparisons will be made with flow-visualization experiments.

Both the experiment and simulations used a Bair Hugger Blower model 750 and an Upper Body Blanket Model 522 to determine the flowrate through the system. Prior experiments found a flowrate of 0.023 kg/s (0.051 lbm/s) for a partially obstructed blanket and 0.025 kg/s (0.055 lbm/s) for a fully open blanket. The lower flow was used in the simulations because of the wrapping of the blanket and surgical draping around the patient.

2. The numerical model

The physical situation is depicted in Figure 1. From the figure, it can be seen that the model fully encompasses an operating room with multiple structures contained therein. The dimensions of the room and the positions of the various components were obtained from a physical measurement of a fully functioning operating room. Details such as the position of lights, the deployment of vents and lighting in the ceiling, the presence of a patient and the surgical draping, various tables, and portions of the exhaust ducts extending into the walls are included in the model.

Figure 2 shows the room with the walls made transparent so that the structures within the airspace can be more easily seen. The patient-warming system used in the simulation is an upper-body blanket that sits atop the patient. The spent air from the blanket was directed toward the patient’s head and

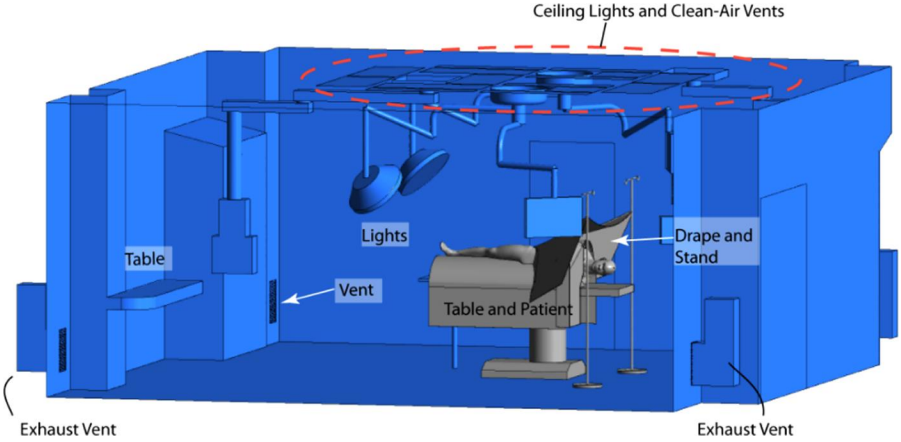


Figure 1. Annotated image of the simulated operation room.

away from the surgical site by the draping. The spent air is isolated from the surgical site by the surgical draping.

The numerical simulations required a subdivision of the air region into a multitude of control volumes. At each control volume, equations conserving mass, energy, and turbulence transport are solved. To achieve accuracy, multiple mesh deployments were used up to approximately 60 million elements. While it is not possible to show all of the elements throughout the room, the projection of elements across the surface is useful for conveying the fineness of the mesh. Figure 3 has been prepared which shows the mesh deployment across the patient's body, the operating table, and the drape. The fineness of the elements makes it difficult to visualize the individual elements.

The boundary conditions consisted of inlet conditions at the ceiling which were a uniformly applied downward volumetric flowrate of $1.1 \text{ m}^3/\text{s}$ ($39 \text{ ft}^3/\text{s}$) with an inlet temperature of 59°F (15°C). The volume of the room is $5,190 \text{ ft}^3$ (147 m^3) so that the ventilation flow resulted in one air change every 130 s. The corresponding mass flowrate is 1.39 kg/s (3.06 lb/s).

The warm air from the forced-convection blanket was treated as a second inlet to the room with temperature of 106°F (41°C) and a flowrate of $0.69 \text{ ft}^3/\text{s}$ ($0.020 \text{ m}^3/\text{s}$). These values were based on experiments carried out using the previously described forced-convection blanket which was also used in the experimental surgical reproduction. In practice, while the temperature leaving the forced-convection heater and entering the blanket is $\sim 109^\circ\text{F}$ (43°C), after it has passed into the blanket and flowed against the patient, it emerges at a lower temperature. Later, to test whether higher patient-warming temperatures may exacerbate buoyant motion, a secondary calculation with 109°F

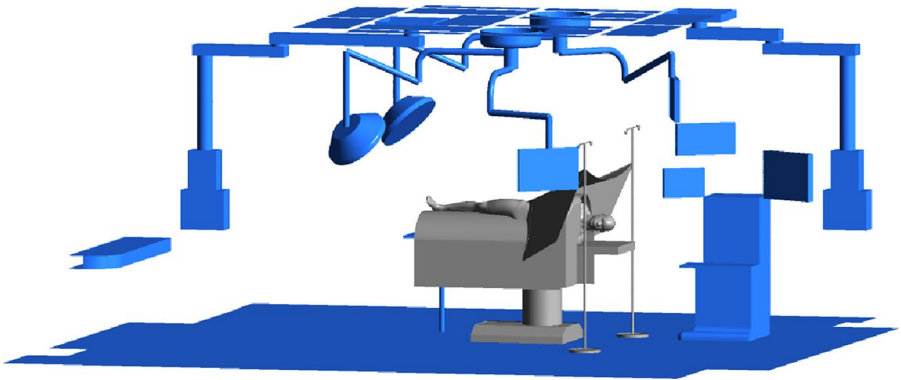


Figure 2. Components within the operating room.

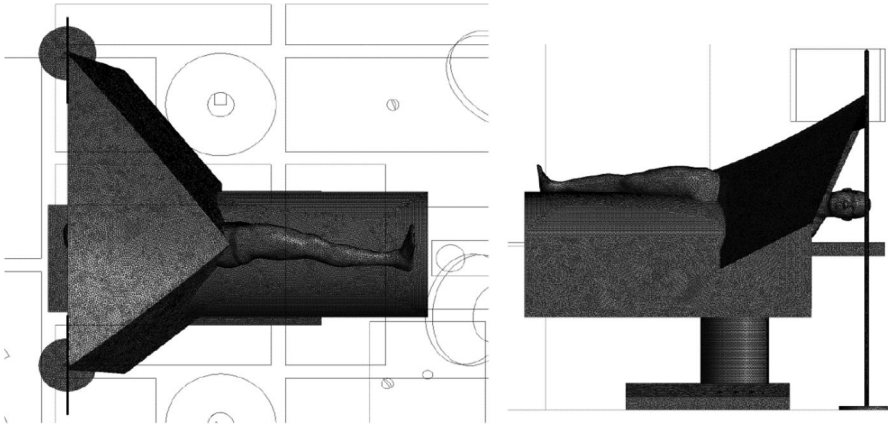


Figure 3. Deployment of the elements along the surgical table, patient, and drape surfaces.

(43°C) was used. In all cases, the fluid was air with a heat capacity of 1,004 J/kg-°C, dynamic viscosity of 1.83×10^{-5} kg/m/s, and thermal conductivity of 0.0261 W/m°C.

At the exits, which were formed by wall-mounted ducting, zero values for the second derivatives of all transported variables were employed. At all surfaces, no-slip adiabatic conditions were employed.

In solving the numerical equations, a Boussinesq approximation was used [106] and interpolation and upwind schemes were employed [107–119]. The treatment of natural convection in enclosures has been an area of active research for many years including recent studies on the subject such as [106,120–154] which deal with computational aspects of buoyancy, the issue of properties, and the potential presence of a forced-convective flow and the potential transport of impurities [155] in the flow. They also provide background on the numerical issues associated with buoyant convection and the potential development of turbulence in such flows. In the literature, comparisons of various turbulent models have been performed [156–159] and on the methodology of variational calculus and interpolation functions in the formulation of the transported equations [160, 161]. Recent studies have quantified the relative importance of the modes of convective and conductive heat transfer for various Rayleigh numbers [162], of the potential of freestream laminar-to-turbulence transition to occur [163–169], and on computational fluid dynamics (CFD) schemes in enclosed mixed convection situations as well as situations where opposing buoyancy characteristics are present in flow [170, 171]. Also considered in this body of work is the unsteady analysis of buoyancy in inclined zones [172, 173] and of buoyant calculations with particles [174].

After careful consideration of the various strengths of numerical approaches, it was decided to use the large-eddy simulation (LES) method because of its capacity to handle complex unsteady flows with buoyancy and eddy formation within the field [175–177]. The LES approach is inherently unsteady and the numerical method separates flow phenomena by spatial scale. The unsteady Navier–Stokes equations are filtered so that eddies whose scales are smaller than the mesh are modeled using a subgrid numerical scheme. The eddy viscosity connects macroscale strain rate to the subgrid stress values. The method differs from regular Reynolds-Averaged Navier–Stokes approaches in that the eddy viscosity selectively represents only the small-scale motion.

While the Smagorinsky model [177] was first developed as an algebraic subgrid scale approach for eddy viscosity, the wall adapted LES model was employed here [178]. This more recent approach has been shown to be superior for reproduction of laminar–turbulent transitions.

For brevity, a full mathematical description of the LES model is not provided here; however, some details are given. A generic filtered variable is defined in the fluid region by

$$\bar{\phi} = \int_{\mathcal{R}} \phi(x') \cdot \gamma(x, x') \cdot dx' \quad (1)$$

where γ is a filtering function that takes on non-zero values within the fluid region and the symbol \Re is the fluid region. The ' symbol represents quantities that are not resolved by the grid scale so that

$$\phi' = \phi - \bar{\phi} \quad (2)$$

The filtered Navier–Stokes equations are then expressed in tensor form as

$$\frac{\partial \bar{u}_i}{\partial t} + \frac{\partial (\bar{u}_i \cdot \bar{u}_j)}{\partial x_j} = -\frac{1}{\rho} \cdot \frac{\partial \bar{p}}{\partial x_i} + \frac{\partial \left(\nu \left(\frac{\partial \bar{u}_i}{\partial x_j} + \frac{\partial \bar{u}_j}{\partial x_i} \right) \right)}{\partial x_j} - \frac{\partial \tau_{ij}}{\partial x_i} \quad (3)$$

where the shear stress are those unresolved at the subgrid scale. They are defined by

$$\tau_{ij} = \bar{u}_i \cdot \bar{u}_j - \bar{u}_i \cdot \bar{u}_j \quad (4)$$

Turbulence at larger scales is solved directly and a subgrid scale eddy viscosity is used for those structures smaller than the grid.

Multiple values of time steps were selected as low as 0.0001 s (resulting in an RMS Courant value of ~ 0.001). The Courant number is defined as

$$Co = \frac{u \cdot \Delta t}{\Delta x} \quad (5)$$

Calculations were continued until a quasi-steady situation was achieved and then further continued with various time-step sizes to ensure numerical accuracy—in total, nearly 3,000 time-step integrations were performed following the achievement of quasi-steady solutions. The transient equations were integrated using a second-order backward Euler scheme, the advection was handled with a high-resolution method [108] and each time step was iterated with a targeted RMS residual of 0.00001 along with an algebraic multi-grid solution acceleration approach [179].

A more coarse numerical approach could have been used if other numerical schemes were employed [180–183]; however, the computationally expensive approach taken here was judged appropriate. The present set of calculations were carried out on a 16-core Dual Xeon E5520 machine with 64 GB RAM and required approximately 55 million CPU seconds (~ 40 days).

The calculation method employed here is well supported in the literature and complements a very active area of research including recent publications dealing with the physics of buoyant and mixed convection, advances to numerical algorithms, improvements in turbulence modeling among others. Interested readers are invited to [184–200] for some very recent papers on these topics.

3. Calculation results and discussion

Insofar as the primary focus of this study is the determination whether air from the warming unit can reach the surgical site, a series of results in that regard is now presented. First, a four-part sequence of images is provided which displays streamlines emerging from the ceiling ventilation and viewed from the foot of the surgical bed (Figure 4). The streamlines are seen passing downward and converging into a coherent structure prior to impacting the surgical table and the floor. After impact with the floor, the flow spreads laterally toward the sidewalls. A complementary view is provided in Figure 5 showing the same streamline images but viewed from the side of the surgical table. It is seen that regardless of the viewing direction, the flow that impacts the surgical site has emanated from the clean air vents positioned in the ceiling.

Since the results of Figures 4 and 5 display streamlines at a particular instance in time, it is relevant to inquire whether the streamline patterns change significantly as time continues to progress. This potential was considered and over 2,000 time steps were made following the achievement of the results already provided. Figure 6 shows four sets of results that correspond to those approximately 900 time steps (Figures 6a, b) and approximately 2,500 time steps (Figures 6c, d). When compared with their counterparts (Figures 4d and 5d), it is seen that there is very little change in the streamlines

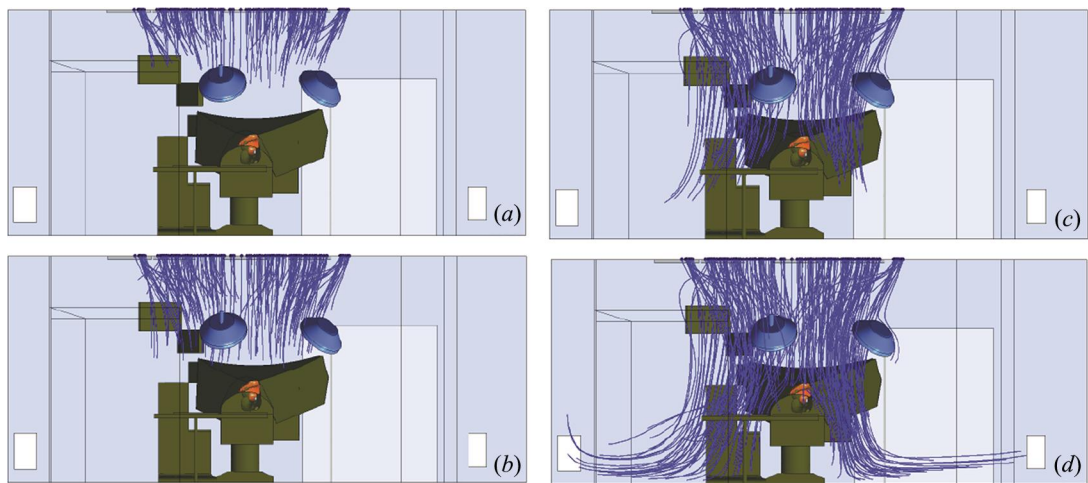


Figure 4. Sequence of images showing the emergence of streamlines from the ceiling ventilation and washing over the operation site, viewed from the foot of a surgical table.

despite the additional calculations. This finding gives further support to the quasi-steady results already presented. These findings clearly show that at no time in the calculation was there an inhibiting of downward air flow which emerges from the ceiling venting in the operating room.

To assess the sensitivity of the calculations to the forced-convection temperature, another calculation was performed. In the new calculation, it was assumed that the air exiting the convection blanket was fixed at 43°C (109 °F). In reality, this is an overestimate of the temperature because the convection air loses heat to the patient and the surroundings. On the other hand, this setting provides an upper bound on the buoyant forces that can be created by the warm air exhaust into the room. The comparison of the previous and new cases is shown in Figure 7. For both views, it is seen that the elevated convection temperature has virtually no impact on the downward air flow.

With issues such as unsteadiness and impacts of exhaust temperature now settled, attention turns toward a deeper examination of the temperature and flow fields for the simulated room. First, Figure 8 has been prepared which shows a temperature contour along a plane which bisects the room

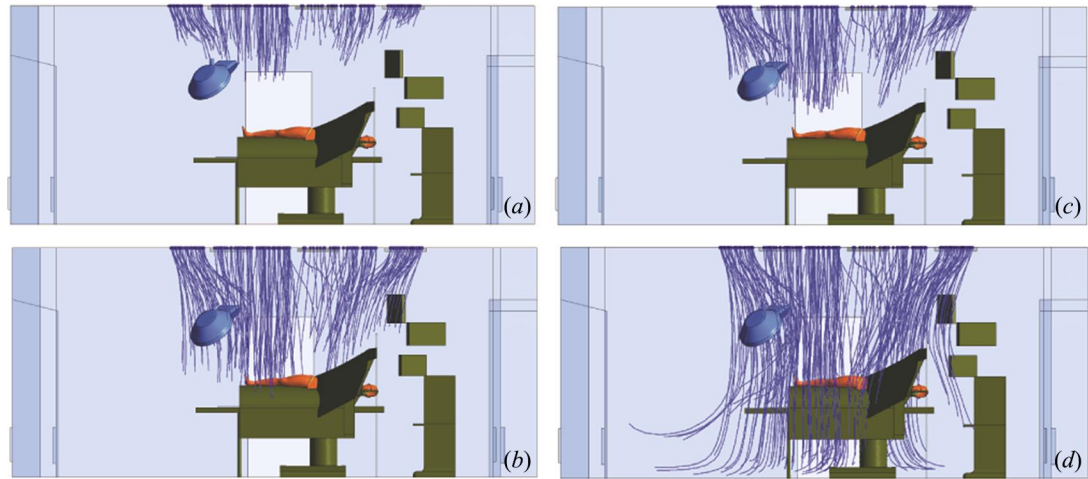


Figure 5. Sequence of images showing the emergence of streamlines from the ceiling ventilation and washing over the operation site, viewed from the side of a surgical table.

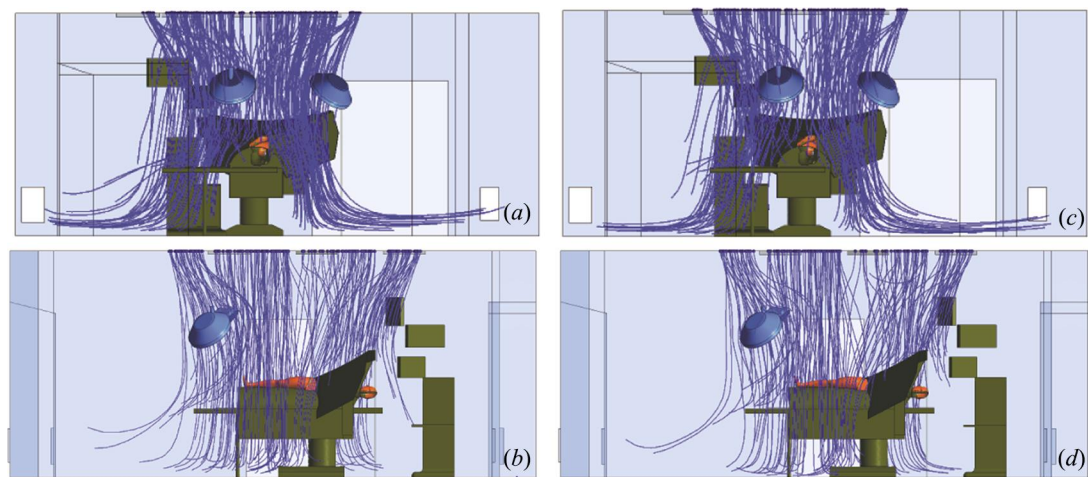


Figure 6. Sequence of images showing the emergence of streamlines from the ceiling ventilation and washing over the operation site. (a) and (b) correspond to approximately 900 time-steps after the attainment of the results of Figures 4 and 5. (c) and (d) correspond to approximately 2,500 time steps following the results of Figures 4 and 5.

and the patient. The plane color is connected with the legend to the left of the image. It is seen that a cool-air plume descends from the ceiling to the patient with some asymmetry. The cool-air downward plume follows the streamline patterns displayed in Figure 4d where the flow was seen to impact the floor and spread laterally toward the bounding walls.

A corollary with Figure 8 is displayed in Figure 9. There, velocity vectors are displayed on the bisecting plane. The vectors are scaled by velocity magnitude so that larger vectors represent faster flow. It is seen that the downward flow slows as it travels horizontally toward the bounding walls. Large-scale eddies form in the room from the entrainment in the ventilation flow. The vectors and temperature contours from Figures 8 and 9 are taken from the quasi-steady solution and are representative of solutions at other times. Any time-wise changes to the solution were negligible.

Insofar as some prior literature suggests that air from the blanket or from beneath the table can be carried by buoyant currents to the surgical site, two other flow pattern results were extracted. The two images, shown together in Figure 10, reveal green streamlines which emerge from the warming

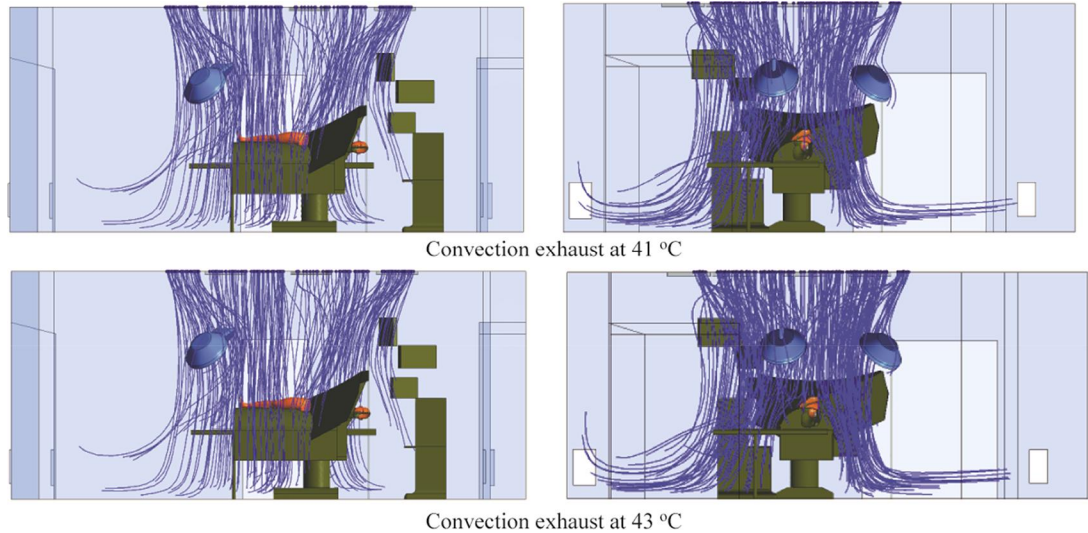


Figure 7. Streamline comparison of foot view and side views of inlet flow for two different exhaust temperatures.

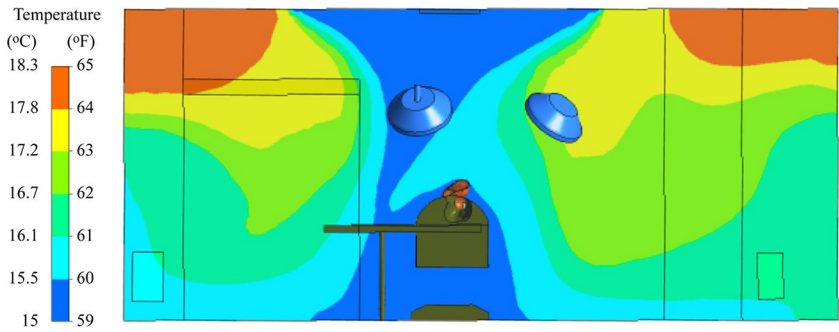


Figure 8. Temperature contour on a bisecting plane viewed from the foot of the surgical bed.

blanket and purple streamlines emerge from underneath the surgical table. In one image, the surgical table is semi-transparent to enable streamlines to be viewed if they passed beneath the table. In the other image, for ease of viewing, the table is opaque. It is seen that in neither case do streamlines emerging from these locations penetrate into the surgical site (area above mannequin hip). The deflection of these streams from the surgical site is accomplished by the downward ventilation flow which has already been described. The meaningfulness of streamlines with respect to the flow in an unsteady situation decreases with distance along a streamline. With this limitation acknowledged, the streamlines of flows shortly after the emergence from the ventilation inlet, the forced warming device, and underneath the table show that in all situations the surgical site was washed by ventilation flow which was effective at deflecting other air sources.

Again, it is recognized that for unsteady flows, streamlines are not necessarily identical with particle pathlines. Consequently, multiple other time instances were evaluated and in no instances did the fluid streamlines impact the surgical site.

One final numerical calculation was performed with the cessation of heated airflow from the convection device. The spent air of the convection device was converted to an adiabatic no-slip wall in the simulation. The results were obtained using the LES method previously described. While approximately 2,000 time-step calculations were completed, virtually no difference was found in the streamline pattern. That is, the room flow patterns with and without the convection device were nearly identical. A graphical image of the inlet streamlines is shown in both foot view and side view in [Figure 11](#).

These numerical results, when considered together, demonstrate that the airflow patterns within the room are dominated by the large downdraft from the inlet vents. The presence or absence of the convection warming device and the actual temperature of the air which emerges from the convection warmer have no significant impact. Furthermore, while the solution is unsteady in nature,

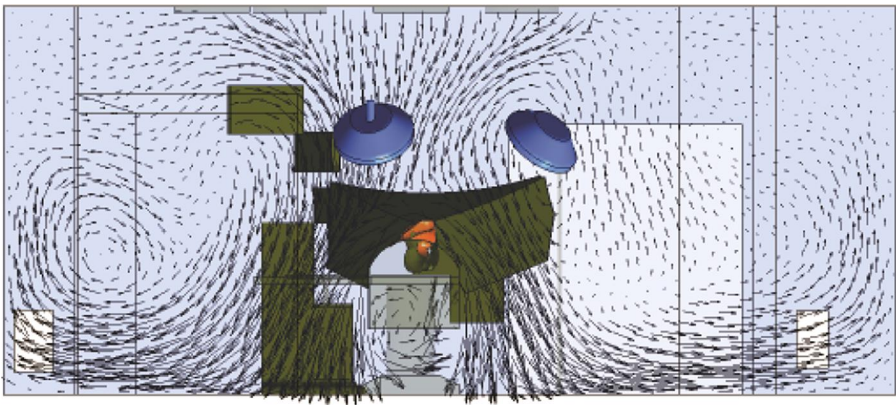


Figure 9. Scaled velocity vectors positioned on the bisecting plane.

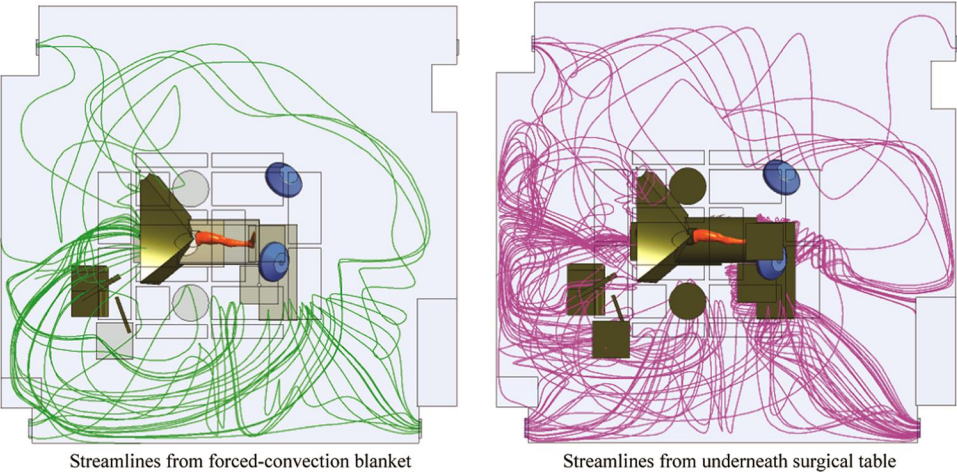


Figure 10. Streamlines emerging from the forced-convection blanket (left) and from beneath the table (right).

the instantaneous streamline patterns, after the emergence from the ventilation inlet, the patient-warming device, or the space underneath the operating table do not vary do not vary significantly. From these results, it is concluded that the convection warming devices do not interrupt normal

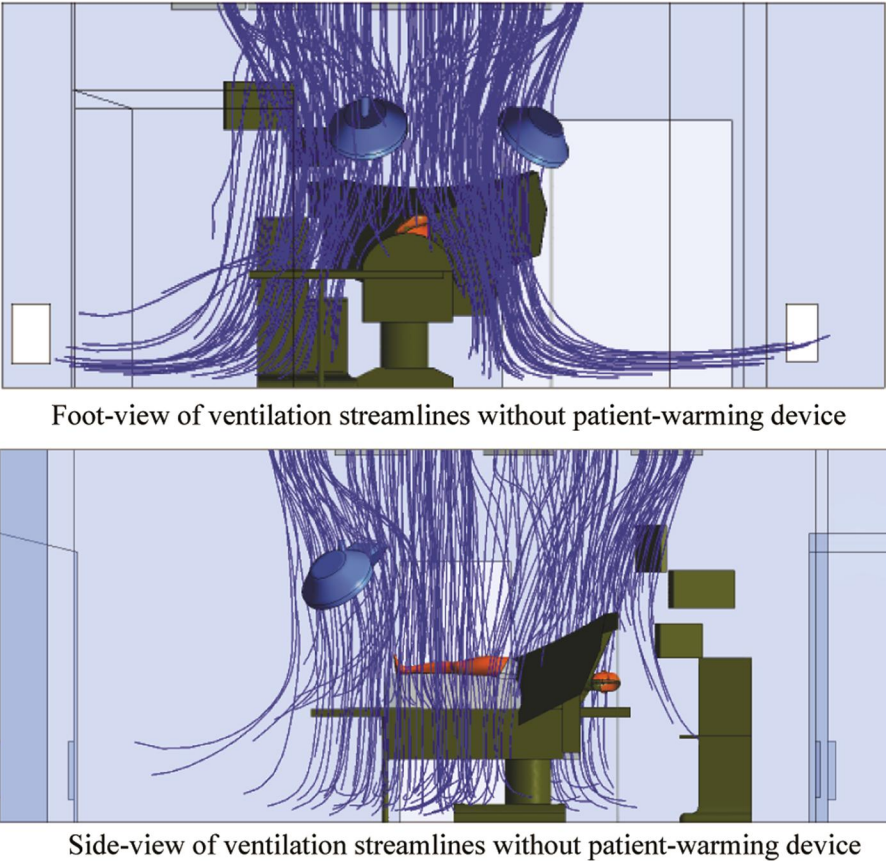


Figure 11. Streamline patterns emerging from the inlet with no forced-convection device.

operating room flow. Furthermore, these model results show no potential that air from the device itself or from beneath the table can be brought to the surgical site.

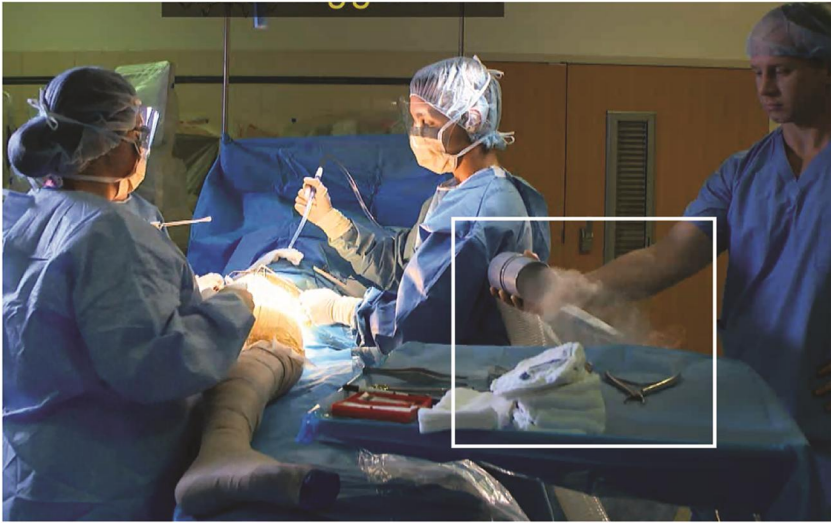
4. Comparison with the experiments

Experiments were performed in the operating room described in the preceding section. While there are inevitable differences between the simulations and the experiments, the close similarity will make meaningful the comparison.

Among the differences is that the experiments were carried out with living humans enacting a simulated surgery. The heat generated by the humans and their movements will impact the airflow in their near vicinity.

In addition, while the measurements used in the numerical simulation were taken from the room, small changes in the positioning of equipment near the wall may influence the flow there. There are other issues such as the uniformity of the flow emerging from the vent or the convection warming system, the fact that the flow visualization was accomplished with vaporized water which has an inherent momentum [exit velocity ~ 1 to 2 ft/s (~ 0.3 to 0.6 m/s)] and potentially some buoyancy (measured fogger temperature 16.9°C (62.5°F)), and other factors which are expected to make imperfect the calculations. Measurements were made of the temperature of the flow exiting the visualization tube; the vaporization device negligibly heated the fluid so that secondary buoyancy was not induced.

The first comparison is made for injected visualization fluid near the knee of the surgical site. [Figure 12](#) shows the photograph from the re-enacted surgery, a white box calls out the injection site. Beneath the main part of the figure, the injection site is repeated along with a partially transparent overlay of black-colored streamlines whose paths are calculated and that emanate from the site. The streamlines are calculated using the instantaneous locus of vector projects at an instant in time.



Black lines are streamlines
calculated from the location of
the flow visualization injector

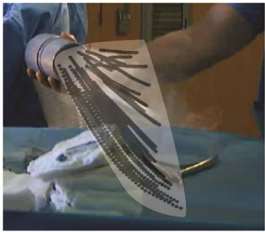


Figure 12. Flow-visualization experiment with the superimposed streamlines from the simulation.

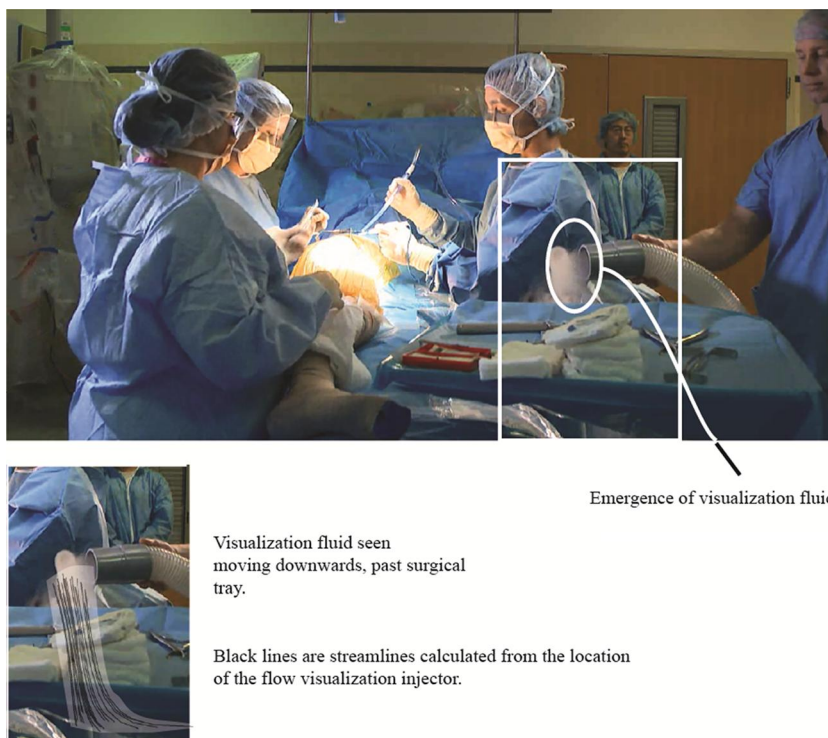


Figure 13. Second flow-visualization experiment with the superimposed streamlines from the numerical simulation.

It is seen that there is excellent agreement in the trajectory of the streamlines and the actual visualization plume.

A second comparison between flow-visualization experiments and the calculated streamline trajectories is made in Figure 13. In the figure, the injection location is closer to the operation site and pointed toward the surgical location. As with Figure 12, a callout is used to identify the injection location. A second image indicates that downward moving flow-visualization fluid can be seen passing vertically behind the surgical table which is in the foreground and between the camera and the injection site. Again, excellent agreement between the injection trajectory and the calculated streamline paths is seen.

Further comparisons were made between temperatures within the room and the calculations. It was found that from the calculations, the room-averaged temperature was 16.7°C (62°F) for an 8.1 million cell calculation. The measurements of the room were 16.1°C (61°F) during the procedure. This is near perfect agreement. The temperature calculated three inches above the floor beneath the patient's head was 15.6°C (60.1°F) and the measurements were 15.9°C (60.5°F) measured in the same location, again near perfect agreement. The temperature at the upper surface at the edge of the bed was measured to be 16.1°C (61°F), whereas temperatures calculated at the same location were 15.7°C (60.3°F). All measurements were made with a type E thin gauge thermocouple wire.

The findings presented here provide strong and direct evidence that buoyant flow patterns caused by a convection patient-warming system do not infringe on the ventilation within an operating room. In particular, in no case was downward clean-air flow patterns disrupted. In fact, in all cases, the air washing over the surgical site was traced to the clean ventilation flow.

5. Concluding remarks

This study was carried out to provide insight about the buoyant airflow patterns within an operating room during a surgical procedure. In particular, one issue studied is whether convection warming

system has the potential to disrupt downward ventilation flow. The calculations used the LES technique and the procedure was subjected to both mesh and time-step independence tests. Boundary conditions and room dimensions were obtained from an operating room which was also used to simulate a surgery.

It was found that the air passing into the surgical site always emanates from the ceiling ventilation. It was also found that warm air which emerges from the convection warming system does not intrude into the surgical site. Nor does air originating from underneath the table pass into the surgical site.

Temperature measurements made within the operating room during the simulated surgery were in near exact agreement with the calculations. In addition, flow patterns obtained by flow-visualization experiments were in agreement with predictions. In fact, patterns of flow-visualization fluid released at two locations near the surgical site showed that air is forced downward and away from the patient. A superposition of the instantaneous streamlines and the flow-visualization pattern was provided.

The results presented here, both from numerical simulation and by experiment, provide mutually reinforcing evidence that convection patient-warming systems do not interfere with operating room ventilation. This study supports the conclusion that concerns of the impact of convection warming on operating room airflow are unsupported and should not result in changes to established clinical practice [201–215].

Acknowledgment

This research was supported by 3 M Corporation.

References

- [1] S. Y. Lyin, H. T. Lai, and C. K. Chen, Hyperthermia Treatment for Living Tissue with Laser Heating Problems by the Differential Transformation Method, *Numer. Heat Transfer A*, vol. 60, pp. 499–518, 2011.
- [2] W. Dai, H. Tu, and R. Nassar, A Fourth-Order Compact Finite-Difference Scheme for Solving a 1D Pennes Bioheat Transfer Equation in a Triple-Layered Skin Structure, *Numer. Heat Transfer B*, vol. 46, pp. 447–461, 2004.
- [3] W. Dai, H. Wang, P. Jordan, R. E. Mickens, and A. Bejan, A Mathematical Model for Skin Burn Injury Induced by Radiation Heating, *Int. J. Heat Mass Transfer*, vol. 51, pp. 5497–5509, 2008.
- [4] R. V. Davalos and B. Rubinsky, Temperature Considerations During Irreversible Electroporation, *Int. J. Heat Mass Transfer*, vol. 51, pp. 5617–5622, 2008.
- [5] M. Jaunich, S. Raje, K. Kim, K. Mitra, and Z. Guo, Bio-Heat Transfer Analysis During Short Pulse Laser Irradiation of Tissues, *Int. J. Heat Mass Transfer*, vol. 51, pp. 5511–5521, 2008.
- [6] J. Sun, A. Zhang, and L. X. Xu, Evaluation of Alternate Cooling and Heating for Tumor Treatment, *Int. J. Heat Mass Transfer*, vol. 51, pp. 5478–5485, 2008.
- [7] H. Vu, O. Garcia-Valladares, and A. Aguilar, Vapor/Liquid Phase Interaction in Flare Flashing Sprays Used in Dermatologic Cooling, *Int. J. Heat Mass Transfer*, vol. 51, pp. 5721–5731, 2008.
- [8] Y. Wang, L. Zhu, and A. J. Rosengart, Targeted Brain Hypothermia Induced by an Interstitial Cooling Device in the Rat Neck: Experimental Study and Model Validation, *Int. J. Heat Mass Transfer*, vol. 51, pp. 5662–5670, 2008.
- [9] M. Shafahi and K. Vafai, Human Eye Response to Thermal Disturbances, *J. Heat Transfer*, vol. 133, paper no. 011009, 2011.
- [10] S. Mahjoob and K. Vafai, Analytical Characterization and Production of an Isothermal Surface for Biological and Electronic Applications, *J. Heat Transfer*, vol. 131, pp. 1–12, 2009.
- [11] M. Iasiello, K. Vafai, A. Andreozzi, N. Bianco, and F. Tavakkoli, Effects of External and Internal Hyperthermia on LDL Transport and Accumulation Within an Arterial Wall in the Presence of a Stenosis, *Ann. Biomed. Eng.*, vol. 43, pp. 1585–1599, 2015.
- [12] K. Wang, F. Tavakkoli, S. Wang, and K. Vafai, Analysis and Analytical Characterization of Bioheat Transfer During Radiofrequency Ablation, *J. Biomech.*, vol. 13, pp. 930–940, 2015.
- [13] I. T. Im, S. B. Youn, and K. Kim, Numerical Study on the Temperature Profiles and Degree of Burns in Human Skin During Combined Thermal Therapy, *Numer. Heat Transfer A*, vol. 67, pp. 921–933, 2015.
- [14] S. J. Beacher, E. M. Sparrow, J. M. Gorman, and J. P. Abraham, Theory and Numerical Simulation of Thermochemical Ablation, *Numer. Heat Transfer A*, vol. 66, pp. 131–143, 2014.
- [15] E. M. Sparrow and J. P. Abraham, A Simulation of Gas-Based, Endometrial-Ablation Therapy for the Treatment of Menorrhagia, *Ann. Biomed. Eng.*, vol. 36, pp. 171–183, 2008.
- [16] J. P. Abraham, E. M. Sparrow, and S. Ramadhyani, Numerical Simulation of a BPH Thermal Therapy—A Case Study Involving TUMT, *J. Biomech. Eng.*, vol. 129, pp. 548–557, 2007.

- [17] N. N. Johnson, J. P. Abraham, Z. I. Helgeson, W. J. Minkowycz, and E. M. Sparrow, An Archive of Skin-Layer Thicknesses and Properties and Calculations of Scald Burns with Comparisons to Experimental Observations, *J. Thermal Science Eng. Appl.*, vol. 3, paper no. 011003, 2011.
- [18] J. P. Abraham, M. P. Hennessey, and W. J. Minkowycz, A Simple Algebraic Model to Predict Burn Depth and Injury, *Int. Comm. Heat Mass Transfer*, vol. 38, pp. 1169–1171, 2011.
- [19] B. L. Vigiianti, M. W. Dewhirst, J. M. Gorman, J. P. Abraham, and E. M. Sparrow, Rationalization of Thermal Injury Quantification Methods: Application to Skin Burns, *Burns*, vol. 40, pp. 896–902, 2014.
- [20] A. Bhowmik, R. Repaka, and S. C. Mishra, Thermal Analysis of the Increasing Subcutaneous Fat Thickness Within the Human Skin—A Numerical Study, *Numer. Heat Transfer A*, vol. 67, pp. 313–329, 2015.
- [21] H. H. Pennes, Analysis of Tissue and Arterial Blood Temperatures in the Resting Human Forearm, *J. Appl. Physiology*, vol. 1, pp. 93–122, 1948.
- [22] M. Fu, W. Weng, and H. Yuan, Numerical Simulation of the Effects of Blood Perfusion, Water Diffusion, and Vaporization on the Skin Temperature and Burn Injuries, *Numer. Heat Transfer A*, vol. 65, pp. 1187–1203, 2014.
- [23] B. W. Raaymakers, A. N. T. J. Kotte, and J. J. W. Lagendijk, Discrete Vasculature (DIVA) Model Simulating the Thermal Impact of Individual Blood Vessels for In Vivo heat Transfer, in W. J. Minkowycz, E. M. Sparrow, and J. P. Abraham (eds.), *Advances in Numerical Heat Transfer*, vol. 3, Taylor and Francis, New York, 2009.
- [24] L. Zhu, T. Schappeler, C. CorderoTumangday, and A. J. Rosengart, Thermal Interactions Between Blood and Tissue, in W. J. Minkowycz, E. M. Sparrow, and J. P. Abraham (eds.), *Advances in Numerical Heat Transfer*, vol. 3, Taylor and Francis, New York, 2009.
- [25] X. Zeng, W. Dai, and A. Bejan, Vascular Countercurrent Network for 3D Triple-Layered Skin Structure with Radiation Heating, *Numer. Heat Transfer A*, vol. 57, pp. 369–391, 2010.
- [26] S. Mahjoob and K. Vafai, Analytical Characterization of Heat Transport through Biological Media Incorporating Hyperthermia Treatment, *Int. J. Heat Mass Transfer*, vol. 52, pp. 1608–1618, 2009.
- [27] A. R. A. Khaled and K. Vafai, The Role of Porous Media in Modeling Flow and Heat Transfer in Biological Tissues, *Int. J. Heat Mass Transfer*, vol. 46, pp. 4989–5003, 2003.
- [28] S. Mahjoob and K. Vafai, Analysis of Heat Transfer in Consecutive Variable Cross-Sectional Domains: Applications in Biological Media and Thermal Management, *J. Heat Transfer*, vol. 133, paper no. 011006, 2011.
- [29] J. W. Baish, K. Mukundakrishnan, and P. S. Ayyaswamy, Numerical Models of Blood Flow Effects in Biological Tissues, in W. J. Minkowycz, E. M. Sparrow, and J. P. Abraham (eds.), *Advances in Numerical Heat Transfer*, vol. 3, Taylor and Francis, New York, 2009.
- [30] J. Zhou and J. Liu, Numerical Study on 3D Light and Heat Transport in Biological Tissues Embedded with Large Blood Vessels During Laser-Induced Thermotherapy, *Numer. Heat Transfer A*, vol. 45, pp. 415–449, 2004.
- [31] J. P. Abraham and E. M. Sparrow, A Thermal Ablation Model Including Liquid-to-Vapor Phase Change, Necrosis-Dependent Perfusion, and Moisture-Dependent Properties, *Int. J. Heat Mass Transfer*, vol. 50, pp. 2537–2544, 2007.
- [32] Z. S. Deng and J. Liu, Numerical Study of the Effects of Large Blood Vessels on Three-Dimensional Tissue Temperature Profiles During Cryosurgery, *Numer. Heat Transfer A*, vol. 49, pp. 47–66, 2006.
- [33] Z. S. Deng and J. Liu, Monte Carlo Method to Solve Multidimensional Bioheat Transfer Problem, *Numer. Heat Transfer B*, vol. 42, pp. 543–567, 2002.
- [34] Q. T. Pham, Finite Element Procedure for Heat Conduction Problems with Internal Heating, *Numer. Heat Transfer A*, vol. 27, pp. 611–619, 2007.
- [35] B. Chen, Y. Gu, and Z. Guan, Nonlinear Transient Heat Conduction Analysis With Precise Time Integration Method, *Numer. Heat Transfer B*, vol. 40, pp. 325–341, 2001.
- [36] F. Moukalled and M. S. Darwish, New Family of Adaptive Very High Resolution Schemes, *Numer. Heat Transfer B*, vol. 4, pp. 215–239, 1998.
- [37] Y. N. Jeng and Z. S. Lee, Revisit to the Modified Multiple One-Dimensional Adaptive Grid Method, *Numer. Heat Transfer B*, vol. 29, pp. 305–323, 1996.
- [38] Y. N. Jeng and Y. C. Lou, Adaptive Grid Generation by Elliptic Equations with Grid Control at All of the Boundaries, *Numer. Heat Transfer B*, vol. 23, pp. 135–151, 1993.
- [39] T. Rhodes and S. Acharya, An Adaptive Differencing Scheme for Flow and Heat Transfer Problems, *Numer. Heat Transfer B*, vol. 23, pp. 153–173, 1993.
- [40] E. Li, G. R. Liu, and V. Tan, Simulation of Hyperthermia Treatment Using the Edge-Based Smoothed Finite-Element Method, *Numer. Heat Transfer A*, vol. 57, pp. 822–847, 2010.
- [41] Z. S. Deng and J. Liu, Numerical Simulation of 3D Freezing and Heating Problems for Combined Cryosurgery and Hyperthermia Therapy, *Numer. Heat Transfer A*, vol. 46, pp. 587–611, 2004.
- [42] N. Afrin, J. Zhou, Y. Zhang, and D. Y. Tzou, Numerical Simulation of Thermal Damage to Living Biological Tissues Induced by Laser Irradiation Based on a Generalized Dual Phase Lag Model, *Numer. Heat Transfer A*, vol. 61, pp. 483–501, 2012.
- [43] B. Bovaheidian and B. Boroomand, Non-Fourier Heat Conduction Problems and the Use of Exponential Basis Functions, *Numer. Heat Transfer A*, vol. 67, pp. 357–379, 2015.

- [44] K. C. Liu and C. T. Lin, Solution of an Inverse Heat Conduction Problem in a Bi-layered Spherical Tissue, *Numer. Heat Transfer A*, vol. 58, pp. 802–818, 2010.
- [45] K. Khanafer and K. Vafai, Synthesis of Mathematical Models Representing Bioheat Transport, in W. J. Minkowycz, E. M. Sparrow, and J. P. Abraham (eds.), *Advances in Numerical Heat Transfer*, vol. 3, Taylor and Francis, New York, 2009.
- [46] A. S. Franca and K. Haghighi, Adaptive Finite Element Analysis of Transient Thermal Problems, *Numer. Heat Transfer B*, vol. 26, pp. 273–292, 1994.
- [47] C. F. Gonzalez Fernandez, F. Alhama, and J. F. Lopez, Application of the Network Method to Heat Conduction Processes with Polynomial and Potential-Exponentially Varying Thermal Properties, *Numer. Heat Transfer A*, vol. 33, pp. 549–559, 1998.
- [48] P. L. Ricketts, A. V. Mudaliar, B. E. Ellis, C. A. Pullins, L. A. Meyers, O. I. Lanz, E. P. Scott, and T. E. Diller, Non-Invasive Blood Perfusion Measurements Using a Combined Temperature and Heat Flux Surface Probe, *Int. J. Heat Mass Transfer*, vol. 51, pp. 5740–5748, 2008.
- [49] L. J. Vallez, B. D. Plourde, and J. P. Abraham, A New Computational Thermal Model for the Whole Human Body: Applications to Patient Warming Blankets, *Numer. Heat Transfer A*, vol. 69, pp. 227–241, 2016.
- [50] E. H. Wissler, Steady-State Temperature Distribution in Man, *J. Appl. Physiol.*, vol. 16, pp. 734–740, 1961.
- [51] E. H. Wissler, Whole-Body Human Thermal Models, in W. J. Minkowycz, E. M. Sparrow, and J. P. Abraham (eds.), *Advances in Numerical Heat Transfer*, vol. 3, pp. 257–306, CRC Press, Boca Raton, FL, 2009.
- [52] K. Khanafer and K. Vafai, Synthesis of Mathematical Models Representing Bioheat Transport, in W. J. Minkowycz and J. P. Abraham (eds.), *Advances in Numerical Heat Transfer*, vol. 3, Chapter 1, pp. 1–28, CRC Press/Taylor & Francis, London, UK, 2009.
- [53] S. H. Xiang and J. Liu, Comprehensive Evaluation on the Heating Capacities of Four Typical Whole Body Hypothermia Strategies Via Compartmental Model, *Int. J. Heat Mass Transfer*, vol. 51, pp. 5486–5496, 2008.
- [54] R. J. Roselli and K. R. Diller KR, *Biotransport: Principles and Applications*, Springer, London, UK, 2011.
- [55] M. Al-Othmani, N. Ghaddar, and K. Ghali, A Multi-Segmented Human Bioheat Model for Transient and Asymmetric Radiative Environments, *Int. J. Heat Mass Transfer*, vol. 51, pp. 5522–5533, 2008.
- [56] H. T. Hammel, Regulation of Internal Body Temperature, *Ann. Rev. Physiology*, vol. 30, pp. 641–710, 1968.
- [57] R. Lenhardt, Monitoring and Thermal Management, *Best Pract. Res. Clin. Anaesthes.*, vol. 17, pp. 569–581, 2003.
- [58] S. R. Insler and D. I. Sessler, Perioperative Thermoregulation and Temperature Monitoring, *Anesthesiol. Clin.*, vol. 24, pp. 823–837, 2006.
- [59] K. Nagashima, Central Mechanisms for Thermoregulation in a Hot Environment, *Ind. Health*, vol. 44, pp. 359–367, 2006.
- [60] J. Gonzalez-Alonso, Human Thermoregulation and the Cardiovascular System, *Exp. Physiol.*, vol. 93, pp. 340–346, 2012.
- [61] J. H. Gibbon and E. M. Landis, Vasodilation in the Lower Extremities in Response to Immersing the Forearms in Warm Water, *J. Clin. Invest.*, vol. 11, pp. 1019–1036, 1932.
- [62] N. E. Freeman, The Effect of Temperature on the Rate of Blood Flow in the Normal and in the Sympathectomized Hand, *Am. J. Physiol.*, vol. 113, pp. 384–398, 1935.
- [63] E. Simon, W. Rautenberg, R. Thauer, and M. Iriki, Auslosung Thermoregulatorischer Reaktionen Durch Locale Kullung im Vertebralkanal, *Naturwissenschaften*, vol. 50, pp. 337, 1963.
- [64] C. Jessen and E. T. Mayer, Spinal Cord and Hypothalamus as Core Sensors of Temperature in the Conscious Dog, I. Equivalence of Responses, *Pflugers Arch.*, vol. 324, pp. 189–204, 1971.
- [65] C. Jessen and O. Ludwig, Spinal Cord and Hypothalamus as Core Sensors of Temperature in the Conscious Dog, II. Addition of Signals, *Pflugers Arch.*, vol. 324, pp. 205–216, 1971.
- [66] C. Jessen and E. Simon, Spinal Cord and Hypothalamus as Core Sensors of Temperature in the Conscious Dog, III. Identity of Functions, *Pflugers Arch.*, vol. 324, pp. 217–226, 1971.
- [67] J. R. S. Hales, A. A. Fawcett, J. W. Bennett, and A. D. Needham, Thermal Control of Blood Flow Through Capillaries and Arteriovenous Anastomoses in Skin of Sheep, *Pflugers Arch.*, vol. 378, pp. 55–63, 1978.
- [68] D. Grahm, J. G. Brock-Utne, D. E. Watenpaugh, and H. C. Heller, Recovery from Mild Hypothermia can be Accelerated by Mechanically Distending Blood Vessels in the Hand, *J. Appl. Physiol.*, vol. 85, pp. 1643–1648, 1998.
- [69] H. C. Heller and D. A. Grahm, Enhancing Thermal Exchange in Humans and Practical Applications, *Disrupt. Sci. Technol.*, vol. 1, pp. 11–19, 2012.
- [70] T. E. Wilson, R. Zhang, B. D. Levine, and C. G. Crandall, Dynamic Autoregulation of Cutaneous Circulation: Differential Control in Glabrous Versus Nonglabrous Skin, *Am. J. Physiol.: Heart Circul. Physiol.*, vol. 289, pp. H385–H391, 2005.
- [71] T. Matsukawa T, D. I. Sessler, A. I. Sessler, M. Schroeder, M. Ozaki, A. Kurz, and C. Cheng, Heat Flow and Distribution During Induction of General Anesthesia, *Anesthesiology*, vol. 82, pp. 662–673, 1995.
- [72] C. Barone, C. Pablo, and G. Barone, Postanesthetic Care in the Critical Care Unit, *Crit. Care Nurse*, vol. 24, pp. 38–45, 2004.

- [73] A. Taguchi, J. Ratnaraj, B. Kabon, N. Sharma, R. Lenhardt, D. I. Sessler, and A. Kurz, Effects of a Circulating-Water Garment and Forced-Air Warming on Body Heat Content and Core Temperature, *Anesthesiology*, vol. 100, pp. 1058–1064, 2004.
- [74] P. Kiekkas and M. Karga, Prewarming: Preventing Intraoperative Hypothermia, *Br. J. Perioperat. Nurs.*, vol. 15, pp. 444–445, 2005.
- [75] K. Good, J. Verble, J. Secrest, and B. Norwood, Postoperative Hypothermia—The Chilling Consequences, *AORN J.*, vol. 83, pp. 1054–1066, 2006.
- [76] S. Cooper, The Effect of Preoperative Warming on Patients' Postoperative Temperatures, *AORN J.*, vol. 83, pp. 1073–1084, 2006.
- [77] J. Andrzejowski, J. Hoyle, G. Eapen, and D. Turnbull, Effect of Prewarming on Post-induction Core Temperature and the Incidence of Inadvertent Perioperative Hypothermia in Patients Undergoing General Anaesthesia, *Br. J. Anaesthesia*, vol. 101, pp. 627–631, 2008.
- [78] T. Weirich, Hypothermia/Warming Protocols: Why are They not widely Used in the OR? *AORN J.*, vol. 87, pp. 333–344, 2008.
- [79] R. Zink and P. A. Iaizzo, Convective Warming Therapy does not Increase the Risk of Wound Contamination in the Operating Room, *Anesth. Analg.*, vol. 76, pp. 50–53, 1993.
- [80] M. S. Avidan, N. Jones, M. Khoosal, C. Lundgren, and D. F. Morrell, Convection Warmers—Not Just Hot Air, *Anaesthesia*, vol. 52, pp. 1073–1076, 1997.
- [81] N. Tumia and G. P. Ashcroft, Convection Warmers—A Possible Source of Contamination in Laminar Airflow Operating Theaters, *J. Hosp. Infect.*, vol. 52, pp. 171–174, 2002.
- [82] R. S. Sharp, T. Chesworth, and E. D. Fern, Do warming Blankets Increase Bacterial Counts in the Operating Field in a Laminar-Flow Theatre? *J. Bone Joint Surg. Br.*, vol. 84-B, pp. 486–488, 2002.
- [83] J. C. K. Huang, E. F. Shah, N. Vinodkumar, M. A. Hegarty, and R. A. Greateorex, The Bair Hugger Patient Warming System in Prolonged Vascular Surgery: An Infection Risk? *Critical Care*, vol. 7, pp. R13–R16, 2003.
- [84] B. Moretti, A. M. V. Larocca, C. Napoli, D. Martinelli, L. Paolillo, M. Cassano, A. Notarnicola, L. Moretti, and V. Pesce, Active Warming Systems to Maintain Perioperative Normothermia in Hip Replacement Surgery: A Therapeutic Aid or a Vector of Infection? *J. Hosp. Infect.*, vol. 73, pp. 58–63, 2009.
- [85] D. I. Sessler, R. N. Olmsted, and R. Kuelpmann, Forced-Air Warming does not Worsen Air Quality in Laminar Flow Operating Rooms, *Anesth. Analg.*, vol. 113, pp. 1416–1420, 2011.
- [86] ECRI Institute, Forced-Air Warming and Surgical Site Infections, *Health Dev.*, pp. 122–125, 2013.
- [87] M. D. Kellam, L. S. Dieckmann, and P. N. Austin, Forced-Air Warming Devices and the Risk of Surgical Site Infections, *AORN*, vol. 98, pp. 353–369, 2013.
- [88] A. Bonner, Evidence is Inconclusive that Forced Air Warming Devices Increase Surgical Site Contamination or Infection, Doctor of Nursing Practice School of Nurse Anesthesia, Texas Christian University, Fort Worth, TX.
- [89] P. Alijanipour, J. Karam, A. Linas, K. Vince, C. Zalavras, M. Austin, and G. Garrigues, Operative Environment, *J. Arthroplasty*, vol. 29, Supplement 1, pp. 49–64, 2014.
- [90] P. N. Austin, The Information Age and Hot Air, *AANA J.*, vol. 83, pp. 237–239, 2015.
- [91] A. T. Bernards, H. I. J. Harinck, L. Dijkshoorn, T. J. K. Van der Reijden, and P. J. Van den Broek, Persistent *Acinebactor baumannii*? Look Inside Your Medical Equipment, *Inf. Control Hosp. Epidemiol.*, vol. 25, pp. 1002–1004, 2004.
- [92] M. Albrecht, R. Gauthier, and D. Leaper, Forced-Air Warming: A Source of Airborne Contamination in the Operating Room? *Orth. Rec.*, vol. 1, no. e28, pp. 85–89, 2009.
- [93] P. D. McGovern, M. Albrecht, K. G. Belani, C. Nachtsheim, P. F. Partington, I. Carluke, and M. R. Reed, Forced-Air Warming and Ultra-Clean Ventilation do not Mix, *J. Bone Joint Surg.*, vol. 93-B, pp. 1537–1544, 2011.
- [94] M. Albrecht, R. L. Gauthier, K. Belani, M. Litchy, and D. Leaper, Forced-Air Warming Blowers: An Evaluation of Filtration Adequacy and Airborne Contamination Emissions in the Operating Room, *Am. J. Inf. Control*, vol. 39, pp. 321–3328, 2011.
- [95] K. B. Dasari, M. Albrecht, and M. Harper, Effect of Forced-Air Warming on the Performance of Operating Theatre Laminar Flow Ventilation, *Anaesthesia*, vol. 67, pp. 244–249, 2012.
- [96] K. G. Belani, M. Albrecht, P. D. McGovern, M. Reed, and C. Nachtsheim, Patient Warming Excess Heat: The Effects on Orthopedic Operating Room Ventilation Performance, *Anesth. Analg.*, vol. 117, pp. 406–411, 2013.
- [97] M. Reed, O. Kimberger, P. D. McGovern, and M. C. Albrecht, Forced-Air Warming Design: Evaluation of Intake Filtration, Internal Microbial Buildup, and Airborne-Contamination Emissions, *AANA J.*, vol. 81, pp. 275–280, 2013.
- [98] A. W. Wood, C. Moss, A. Keenan, M. R. Reed, and D. J. Leaper, Infection Control Hazards Associated with the Use of Forced-Air Warming in Operating Theatres, *J. Hospital Inf.*, vol. 88, pp. 132–140, 2014.
- [99] A. J. Legg, T. Cannon, and A. J. Hamer, Do Forced Air Patient-Warming Devices Disrupt Unidirectional Downward Airflow? *Arthroplasty*, vol. 94-B, pp. 254–256, 2012.
- [100] A. J. Legg and A. J. Hamer, Forced-Air Patient Warming Blankets Disrupt Unidirectional Airflow, *Bone Joint J.*, vol. 95-B, pp. 407–410, 2013.
- [101] Q. Chen, Z. Jiang, and A. Moser, Control of Airborne Particle Concentration and Draught Risk in an Operating Room, *Indoor Air*, vol. 2, pp. 154–167, 1992.

- [102] F. Memarzadeh and A. P. Manning, Comparison of Operating Room Ventilation Systems in the Protection of the Surgical Site, *ASHRAE Trans.*, vol. 108, pp. 4549–4552, 2002.
- [103] F. Memarzadeh and Z. Jiang, Effect of Operating Room Geometry and Ventilation System Parameter Variations on the Protection of the Surgical Site, *Proceedings of IAQ 2004*, Tampa Bay, FL.
- [104] F. Romano, L. K. Marocco, J. Gusten, and C. M. Joppolo, Numerical and Experimental Analysis of Airborne Particles Control in an Operating Theater, *Build. Environ.*, vol. 89, pp. 369–379, 2015.
- [105] Z. I. Helgeson, J. Jenkins, J. P. Abraham, and E. M. Sparrow, Particle Trajectories and Agglomeration/Accumulation in Branching Arteries Subjected to Orbital Atherectomy, *Open Biomed. Eng. J.*, vol. 5, pp. 25–38, 2011.
- [106] E. M. Sparrow and J. P. Abraham, A New Buoyancy Model Replacing the Standard Pseudo-Density Difference for Internal Natural Convection in Gases, *Int. J. Heat Mass Transfer*, vol. 46, pp. 3583–3591, 2003.
- [107] S. Majumdar, Role of Underrelaxation in Momentum Interpolation for Calculation of Flow with Nonstaggered Grids, *Numer. Heat Transfer*, vol. 13, pp. 125–132, 1988.
- [108] T. J. Barth and D. C. Jespersen, The Design and Applications of Upwind Schemes on Unstructured Meshes, AIAA Paper no. 89–03, 1989.
- [109] F. Wang, W. Zhang, S. Y. Lv, C. T. Huang, and L. Liu, Fourier Analysis of the Effect of Grid Non-Orthogonality on the SIMPLE Algorithm, *Numer. Heat Transfer B*, vol. 67, pp. 531–549, 2015.
- [110] A. Ashrafizadeh, B. Alinia, and P. Mayeli, A New Co-Located Pressure Based Discretization Method for the Numerical Solution of Incompressible Navier-Stokes Equations, *Numer. Heat Transfer B*, vol. 67, pp. 563–589, 2015.
- [111] D. K. Kolmogorov, W. Z. Shen, N. N. Sorensen, and J. N. Sorensen, Fully Consistent SIMPLE-Like Algorithms on Collocated Grids, *Numer. Heat Transfer B*, vol. 67, pp. 101–123, 2015.
- [112] N. S. C. Kao, T. W. H. Sheu, and S. F. Tsai, On a Wavenumber Optimized Streamline Upwinding Method for Solving Incompressible Navier-Stokes Equations, *Numer. Heat Transfer B*, vol. 67, pp. 75–99, 2015.
- [113] P. Roy, N. K. Anand, and D. Donzis, A Parallel-Multigrid Finite-Volume Solver on a Collocated Grid for Incompressible Navier-Stokes Equations, *Numer. Heat Transfer B*, vol. 67, pp. 376–409, 2015.
- [114] K. K. Q. Zhang, B. Shotoerban, W. J. Minkowycz, and F. Mashayek, A Compact Finite Difference Method on Staggered Grid for Navier-Stokes Flows, *Int. J. Numer. Meth. Fluids*, vol. 52, pp. 867–881, 2006.
- [115] K. M. Kelkar, D. Choudhury, and W. J. Minkowycz, Numerical Method for the Computational of Flow in Irregular Domains that Exhibit Geometric Periodicity Using Non-Staggered Grids, *Numer. Heat Transfer*, vol. 31, pp. 1–12, 1997.
- [116] K. K. Q. Zhang, B. Rovagnati, Z. Gao, W. J. Minkowycz, and F. Mashayek, An Introduction to the Lattice Grid, *Numer. Heat Transfer B*, vol. 51, pp. 415–431, 2007.
- [117] G. Comini, W. J. Minkowycz, and W. Shyy, General Algorithms for the Finite Element Solution of Incompressible Flow Problems Using Primitive Variables, *Adv. Numer. Heat Transfer*, vol. 1, pp. 137–139, 1996.
- [118] T. M. Shi, L. J. Hayes, W. J. Minkowycz, K. T. Yang, and W. Aung, Parallel Computations in Heat Transfer, *Numer. Heat Transfer*, vol. 9, pp. 639–662, 1986.
- [119] T. C. Chawla, G. Leaf, and W. J. Minkowycz, A Collocation Method for Convection Dominated Flows, *Int. J. Numer. Meth. Fluids*, vol. 4, pp. 271–281, 1984.
- [120] G. Yang and J. Y. Wu, Effects of Natural Convection, Wall Thermal Conduction, and Thermal Radiation Radiation on Heat Transfer Uniformity at a Heated Plate Located at the Bottom of a Three-Dimensional Rectangular Enclosure, *Numer. Heat Transfer A*, vol. 69, pp. 589–606, 2016.
- [121] M. A. Sheremet and I. V. Miroshnichenko, Effect of Surface Radiation on Transient Natural Convection in a Wavy-Walled Cavity, *Numer. Heat Transfer A*, vol. 69, pp. 369–382, 2016.
- [122] J. Wu, P. Huang, and X. Feng, A New Variational Multiscale FEM for the Steady-State Natural Convection Problem with Bubble Stabilization, *Numer. Heat Transfer A*, vol. 68, pp. 777–796, 2015.
- [123] S. M. Dash and T. S. Lee, Natural Convection in a Square Enclosure with a Square Heat Source at Two Different Horizontal and Diagonal Eccentricities, *Numer. Heat Transfer A*, vol. 68, pp. 686–710, 2015.
- [124] F. Wu, G. Wang, and W. Zhou, A Thermal Nonequilibrium Approach to Natural Convection in a Square Enclosure Due to Partially Cooled Sidewalls of the Enclosure, *Numer. Heat Transfer A*, vol. 67, pp. 771–790, 2015.
- [125] T. Rasool, A. Dhiman, and M. Parveez, Cross-Buoyancy Mixed Convection Around a Confined Triangular Body, *Numer. Heat Transfer A*, vol. 76, pp. 454–475, 2015.
- [126] J. P. Dulhani and A. Dala, Flow Past an Equilateral Triangular Bluff Obstacle: Computational Study of the Effect of Thermal Buoyancy on Flow Physics and Heat Transfer, *Numer. Heat Transfer A*, vol. 67, pp. 476–495, 2015.
- [127] Z. Huang, W. Zhang, and G. Xi, Natural Convection Heat Transfer in a Cubic Cavity Submitted to Time-Periodic Sidewall Temperature, *Numer. Heat Transfer A*, vol. 67, pp. 13–32, 2015.
- [128] X. Yuan, F. Tavakkoli, and K. Vafai, Analysis of Natural Convection in Horizontal Concentric Annuli of Varying Inner Shape, *Numer. Heat Transfer A*, vol. 68, pp. 1155–1174, 2015.
- [129] R. Ellahi, A. Riaz, S. Abbasbandy, T. Hayat, and K. Vafai, A Study on the Mixed Convection Boundary Layer Flow and Heat Transfer Over a Vertical Slender Cylinder, *J. Thermal Sci.*, vol. 18, pp. 1247–1258, 2014.

- [130] A. Haghighi and K. Vafai, Optimal Positioning of Strips for Heat Transfer Reduction within an Enclosure, *Numer. Heat Transfer A*, vol. 66, pp. 17–14, 2014.
- [131] W. Shi and K. Vafai, Mixed Convection in an Obstructed Open-ended Cavity, *Numer. Heat Transfer A*, vol. 57, pp. 709–729, 2010.
- [132] M. Manca, S. Nardini, and K. Vafai, Experimental Analysis of Opposing Flow in Mixed Convection in a Channel with an Open Cavity Below, *Exp. Heat Transfer J.*, vol. 21, pp. 99–114, 2008.
- [133] O. Manca, S. Nardini, K. Khanafer, and K. Vafai, Effect of Heated Wall Position on Mixed Convection in a Channel with an Open Cavity, *Numer. Heat Transfer A*, vol. 43, pp. 259–282, 2003.
- [134] K. Khanafer, K. Vafai, and M. Lightstone, Mixed Convection Heat Transfer in Two-Dimensional Open-Ended Enclosures, *Int. J. Heat Mass Transfer*, vol. 45, pp. 5171–5190, 2002.
- [135] K. Khanafer and K. Vafai, Effective Boundary Conditions for Buoyancy-driven Flows and Heat Transfer in Fully Open-Ended Two-Dimensional Enclosures, *Int. J. Heat Mass Transfer*, vol. 45, pp. 2527–2538, 2002.
- [136] K. Vafai and J. Ettefagh, Thermal and Fluid Flow Instabilities in Buoyancy-Driven Flows in Open-Ended Cavities, *Int. J. Heat Mass Transfer*, vol. 33, pp. 2329–2344, 1990.
- [137] M. P. Dyko and K. Vafai, Effects of Gravity Modulation on Convection in a Horizontal Annulus, *Int. J. Heat Mass Transfer*, vol. 50, pp. 348–360, 2007.
- [138] A. R. A. Khaled and K. Vafai, Heat Transfer and Flow Induced by Both Natural Convection and Vibrations Inside an Open-End Vertical Channel, *Heat and Mass Transfer*, vol. 40, pp. 325–337, 2004.
- [139] A. Ali, K. Vafai, and A. R. A. Khaled, Analysis of Heat and Mass Transfer Between Air and Falling in a Cross Flow Configuration, *Int. J. Heat Mass Transfer*, vol. 47, pp. 743–755, 2004.
- [140] K. Khanafer, K. Vafai, and M. Lightstone, Buoyancy-Driven Heat Transfer Enhancement in a Two-Dimensional Enclosure Utilizing Nanofluids, *Int. J. Heat Mass Transfer*, vol. 46, pp. 3639–3653, 2003.
- [141] W. J. Minkowycz and C. Ping, Free Convection About a Vertical Cylinder Embedded in a Porous Medium, *Int. J. Heat Mass Transfer*, vol. 19, pp. 805–813, 1976.
- [142] M. P. Dyko, K. Vafai, and A. K. Mojtabi, Numerical and Experimental Investigation of Stability of Natural Convective Flows Within a Horizontal Annulus, *J. Fluid Mech.*, vol. 381, pp. 27–61, 1999.
- [143] M. P. Dyko and K. Vafai, Fundamental Issues and Recent Advancements in Analysis of Aircraft Brake Natural Convective Cooling, *J. Heat Transfer*, vol. 120, pp. 840–857, 1998.
- [144] C. P. Desai and K. Vafai, Experimental and Numerical Study of Buoyancy Induced Flow and Heat Transfer in an Open Annular Cavity, *Int. J. Heat Mass Transfer*, vol. 39, pp. 2053–2066, 1996.
- [145] K. Vafai and S. J. Kim, Discussion on Forced Convection in a Porous Channel with Localized Heat Sources, *J. Heat Transfer*, vol. 117, pp. 1097–1098, 1995.
- [146] C. P. Desai, K. Vafai, and M. Keyhani, On the Natural Convection in a Cavity with a Cooled Top Wall and Multiple Protruding Heaters, *J. Electron. Packag.*, vol. 117, pp. 34–45, 1995.
- [147] E. M. Sparrow and W. J. Minkowycz, Buoyancy Effects on Horizontal Boundary-Layer Flow and Heat Transfer, *Int. J. Heat Mass Transfer*, vol. 5, pp. 505–511, 1962.
- [148] J. P. Abraham and E. M. Sparrow, Three Dimensional Laminar and Turbulent Natural Convection in a Continuously/Discretely Wall-Heated Enclosure Containing a Thermal Load, *Numer. Heat Transfer A*, vol. 44, pp. 105–125, 2003.
- [149] E. M. Sparrow and J. P. Abraham, Heat Transfer Coefficients and Other Performance Parameters for Variously Positioned and Supported Thermal Loads in Ovens With/Without Water-Filled or Empty Blockages, *Int. J. Heat Mass Transfer*, vol. 45, pp. 3597–3607, July 2002.
- [150] W. J. Minkowycz and E. M. Sparrow, Local Nonsimilar solutions for Natural Convection on a Vertical Cylinder, *J. Heat Transfer*, vol. 96, pp. 178–183, 1974.
- [151] M. A. Sheremet, Unsteady Conjugate Natural Convection in a Three-Dimensional Enclosure Porous, *Numer. Heat Transfer A*, vol. 68, pp. 243–267, 2015.
- [152] M. A. Ismael and A. J. Chamkha, Mixed Convection in Lid-Driven Trapezoidal Cavities with an Aiding or Opposing Side Wall, *Numer. Heat Transfer A*, vol. 68, pp. 312–335, 2015.
- [153] Q. Pelletier, D. B. Murray, and T. Persoons, Unsteady Natural Convection Heat Transfer from a Pair of Vertically Aligned Horizontal Cylinders, *Int. J. Heat Mass Transfer*, vol. 95, pp. 693–708, 2016.
- [154] M. Roy, T. Basak, S. Roy, and I. Pop, Analysis of Entropy Generation for Mixed Convection in a Square Cavity for Various Thermal Boundary Conditions, *Numer. Heat Transfer A*, vol. 68, pp. 44–74, 2015.
- [155] L. V. Matveev, Impurity Transport in Developed Rayleigh-Bernard Convection, *Int. J. Heat Mass Transfer*, vol. 95, pp. 15–21, 2016.
- [156] S. K. Rathore and M. K. Das, Numerical Investigation on the Performance of Low-Reynolds Number k-e Model for Buoyancy-Opposed Wall Jet Flow, *Int. J. Heat Mass Transfer*, vol. 95, pp. 636–649, 2016.
- [157] W. Li, J. Ren, J. Hongde, and P. Ligrani, Assessment of Six Turbulence Models for Modeling and Predicting Narrow Passage Flows, Part 1: Impingement Jets, *Numer. Heat Transfer A*, vol. 69, pp. 109–127, 2016.
- [158] A. Keshmiri, J. Uribe, and N. Shokri, Benchmarking of Three Different CFD Codes in Simulating Natural, Forced and Mixed Convection Flows, *Numer. Heat Transfer A*, vol. 67, pp. 1324–1351, 2015.

- [159] A. Javadi, M. Pasandideh-Fard, and M. Malek-Jafarian, Modification of k- ϵ Turbulent Model Using Kinetic Energy-Preserving Method, *Numer. Heat Transfer B*, vol. 67, pp. 554–577, 2015.
- [160] H. Xiang and X. Zhang, Variational Multiscale Element-Free Galerkin Method and Precise Time Step Integration Method for Convection Diffusion Problems, *Numer. Heat Transfer A*, vol. 67, pp. 210–223, 2015.
- [161] D. Pan, A High-Order Piecewise Polynomial Reconstruction for Finite-Element Methods Solved Convection and Diffusion Equations, *Numer. Heat Transfer B*, vol. 67, pp. 495–510, 2015.
- [162] F. Moukalled, M. Darwish, K. Kasamani, A. Hammoud, and M. K. Mansour, Buoyancy-Induced Flow and Heat Transfer in a Porous Annulus Between Concentric Horizontal Circular and Square Cylinders, *Numer. Heat Transfer A*, vol. 69, pp. 1029–1050, 2016.
- [163] J. P. Abraham, J. C. K. Tong, and E. M. Sparrow, Breakdown of Laminar Pipe Flow into Transitional Intermittency and Subsequent Attainment of Fully Developed Intermittent or Turbulent Flow, *Numer. Heat Transfer B*, vol. 54, pp. 103–115, 2008.
- [164] J. P. Abraham, E. M. Sparrow, and J. C. K. Tong, Heat Transfer in All Pipe Flow Regimes—Laminar, Transitional/Intermittent, and Turbulent, *Int. J. Heat Mass Transfer*, vol. 52, pp. 557–563, 2009.
- [165] W. J. Minkowycz, J. P. Abraham, and E. M. Sparrow, Numerical Simulation of Laminar Breakdown and Subsequent Intermittent and Turbulent Flow in Parallel Plate Channels: Effects of Inlet Velocity Profile and Turbulence Intensity, *Int. J. Heat Mass Transfer*, vol. 52, pp. 4040–4046, 2009.
- [166] R. D. Lovik, J. P. Abraham, W. J. Minkowycz, and E. M. Sparrow, Laminarization and Turbulentization in a Pulsatile Pipe Flow, *Numer. Heat Transfer A*, vol. 56, pp. 861–879, 2009.
- [167] J. P. Abraham, E. M. Sparrow, J. C. K. Tong, and D. W. Bettenhausen, Internal Flows which Transist from Turbulent Through Intermittent to Laminar, *Int. J. Thermal Sci.*, vol. 49, pp. 256–263, 2010.
- [168] J. P. Abraham, E. M. Sparrow, and W. J. Minkowycz, Internal-Flow Nusselt Numbers for the Low-Reynolds-Number End of the Laminar-to-Turbulent Transition Regime, *Int. J. Heat Mass Transfer*, vol. 54, pp. 584–588, 2011.
- [169] Keshmiri, A. Revell and H. G. Darabkhani, Assessment of a Common Nonlinear Eddy-Viscosity Turbulence Model in Capturing Laminarization in Mixed Convection Flows, *Numer. Heat Transfer A*, vol. 69, pp. 146–165, 2016.
- [170] R. Duan, W. Liu, L. Xu, Y. Huang, X. Shen, C. H. Lin, J. Liu, Q. Chen, and B. Sansanapuri, Mesh Type and Number for the CFD Simulations of Air Distribution in an Aircraft Cabin, *Numer. Heat Transfer B*, vol. 67, pp. 489–5076, 2015.
- [171] D. Kumar and A. Dhiman, Opposing Buoyancy Characteristics of Newtonian Fluid Flow Around a Confined Square Cylinder at Low and Moderate Reynolds Number, *Numer. Heat Transfer A*, vol. 69, pp. 874–897, 2016.
- [172] A. Bairi and O. Haddad, Detailed Correlations on Natural Convective Heat Transfer Coefficients for QFN32 Electronic Device on Inclined PCV, *Numer. Heat Transfer A*, vol. 69, pp. 841–849, 2016.
- [173] M. M. Rahman, H. F. Oztog, A. H. Joarder, R. Saidur, N. Hamzah, K. Al-Salen, and T. A. Ibrahim, Unsteady Analysis of Natural Convection in a Carbon Nanotube-Water Filled Cavity with Inclined Heater, *Numer. Heat Transfer A*, vol. 69, pp. 794–809, 2016.
- [174] A. K. Gupta and R. P. Chhabra, Mixed Convection from a Spheroid in Bingham Plastic Fluids: Effect of Buoyancy-Assisted Flow, *Numer. Heat Transfer A*, vol. 69, pp. 898–920, 2016.
- [175] S. M. Yahya, S. F. Anwer, and S. Sanghi, LES of Stably Stratified Flow with Varying Thermophysical Properties, *Numer. Heat Transfer A*, vol. 67, pp. 1408–1427, 2015.
- [176] A. C. Yuen, G. H. Yeoh, V. Timochenko, and T. Barber, LES and Multi-Step Chemical Reaction in Compartment Fires, *Numer. Heat Transfer A*, vol. 68, pp. 711–736, 2015.
- [177] J. Smagorinsky, General Circulation Experiments with Primitive Equations, *Mon. Weather Rev.*, vol. 93, pp. 99–165, 1963.
- [178] F. Nicoud and F. Ducros, Subgrid-Scale Stress Modeling Based on the Square of the Velocity Gradient Tensor, *Flow Turbul. Combust.*, vol. 62, pp. 183–200, 1999.
- [179] M. J. Raw, Robustness of Coupled Algebraic Multigrid for Solving Navier Stokes Equations, *AIAA 34th Aerospace and Sciences Meeting and Exhibit*, Reno, NV, January 15–18, 1996.
- [180] D. M. S. Albuquerque, J. M. C. Pereira, and J. C. F. Pereira, Residual Least-Squares Error Estimate for Unstructured h-Adaptive Meshes, *Numer. Heat Transfer B*, vol. 67, pp. 187–210, 2015.
- [181] N. S. C. Kao, T. W. H. Sheu, and S. F. Tsai, On a Wavenumber Optimized Streamline Upwinding Method for Solving Steady Incompressible Navier-Stokes Equations, *Numer. Heat Transfer B*, vol. 67, pp. 75–99, 2015.
- [182] Y. Liu, F. Wang, and Y. T. Li, Fourier Analysis of the SIMPLE Serials, *Numer. Heat Transfer B*, vol. 69, pp. 1–20, 2016.
- [183] S. Zhai and X. Feng, A Block-Centered Finite-Difference Method for the Time-Fractional Diffusion Equation on Nonuniform Grids, *Numer. Heat Transfer B*, vol. 69, pp. 217–233, 2016.
- [184] J. M. Gorman, E. M. Sparrow, J. P. Abraham, and W. J. Minkowycz, Evaluation of the Efficacy of Turbulence Models for Swirling Flows and Effect of Turbulence Intensity on Heat Transfer, *Numer. Heat Transfer B*, vol. 70, pp. 485–502, 2016.

- [185] P. S. Cumber, Micromixing Model Performance for Nonreacting Flows Using a Consistent Monte Carlo Method, *Numer. Heat Transfer B*, vol. 70, pp. 517–536, 2016.
- [186] M. A. Sekachev, A. J. Baker, and K. L. Wong, Totally Analytical Closure of Space Filtered Navier-Stokes for Arbitrary Reynolds Number: Part I. Theory, Resolutions, *Numer. Heat Transfer B*, vol. 70, pp. 267–283, 2016.
- [187] M. A. Sekachev, A. J. Baker, and K. L. Wong, Totally Analytical Closure of Space Filtered Navier-Stokes for Arbitrary Reynolds Number: Part II. Resolutions, Algorithms, Validations, *Numer. Heat Transfer B*, vol. 70, pp. 267–283, 2016.
- [188] M. A. Sekachev, A. J. Baker, and K. L. Wong, Totally Analytical Closure of Space Filtered Navier-Stokes for Arbitrary Reynolds Number: Part III. aFNS Theory Validation, *Numer. Heat Transfer B*, vol. 70, pp. 267–283, 2016.
- [189] C. H. Marchi, F. F. Giacomini, and C. D. Santiago, Repeated Richardson Extrapolation to Reduce the Field Discretization Error in Computational Fluid Dynamics, *Numer. Heat Transfer B*, vol. 70, pp. 340–353, 2016.
- [190] M. Angelino, A. Boghi, and F. Gori, Numerical Solution of Three-Dimensional Rectangular Submerged Jets with Evidence of the Undisturbed Region of Flow, *Numer. Heat Transfer A*, vol. 70, pp. 815–830, 2016.
- [191] S. A. Tkachenko, G. E. Lau, V. Timchenko, G. H. Yeoh, and J. Reizes, Effect of Heat Loss on Turbulent Buoyancy-Driven Flow in a Rectangular Cavity Use the Large Eddy Simulation, *Numer. Heat Transfer A*, vol. 70, pp. 689–706, 2016.
- [192] S. Husain and M. A. Siddiqui, Experimental and Numerical Analyses of Natural Convection Flow in a Partially Heated Vertical Annulus, *Numer. Heat Transfer A*, vol. 70, pp. 763–775, 2016.
- [193] R. M. Cotta, C. P. Naveira-Cotta, and D. C. Knupp, Enhanced Convergence of Eigenfunction Expansions in Convection-Diffusion with Multiscale Space Variables, *Numer. Heat Transfer A*, vol. 70, pp. 495–512, 2016.
- [194] P. Zhang, X. Zhang, H. Xiang, and L. Song, A Fast and Stabilized Meshless Method for the Convection Dominated Convection Diffusion Problems, *Numer. Heat Transfer A*, vol. 70, pp. 420–431, 2016.
- [195] C. Sui, F. Yang, and W. Kong, Large Eddy Simulation of Methane/Air Lifted Flame with Hot Co-Flow, *Numer. Heat Transfer A*, vol. 70, pp. 282–292, 2016.
- [196] J. Waters and D. B. Carrington, A Parallel Large Eddy Simulation in a Finite Element Projection Method for All Flow Regimes, *Numer. Heat Transfer A*, vol. 70, pp. 117–131, 2016.
- [197] J. H. Zhang, D. D. Zhang, F. Y. Zhao, and D. Liu, Nonunique Steady Flow Solutions for Pressure Correction Equations Applied in the Regime of Natural Convection Inside Free Vented Enclosures, *Numer. Heat Transfer A*, vol. 70, pp. 145–161, 2016.
- [198] D. Kumar and A. Dhiman, Computations of Newtonian Fluid Flow Around a Square Cylinder Near and Adiabatic Wall at Low and Intermediate Reynolds Numbers: Effects of Cross-Buoyancy and Mixed Convection, *Numer. Heat Transfer A*, vol. 70, pp. 162–186, 2016.
- [199] R. P. Soni and M. R. Gavara, Natural Convection in a Cavity Surface mounted with Discrete Heaters and Subjected to Different Cooling Configurations, *Numer. Heat Transfer A*, vol. 70, pp. 79–102, 2016.
- [200] K. Zhang, L. Wang, and Y. Zhang, Improved Finite Difference Method with Compact Correction Term for Solving Poisson's Equations, *Numer. Heat Transfer B*, vol. 70, pp. 393–405, 2016.
- [201] R. L. Lennon, M. P. Hosking, M. A. Conover, and W. J. Perkins, Evaluation of a Forced-Air System for Warming Hypothermic Postoperative Patients, *Anesth Anal.*, vol. 70, pp. 424–427, 1990.
- [202] G. G. Giesbrecht, M. B. Ducharme, and J. P. McGuire, Comparison of Forced-Air Patient Warming Systems of Perioperative Use, *Anesthesiology*, vol. 80, pp. 671–679, 1994.
- [203] A. Kurz, D. I. Sessler, and R. Lenhardt, Perioperative Normothermia to Reduce the Incidence of Surgical-Wound Infection and Shorten Hospitalization, *N. Engl. J. Med.*, vol. 334, pp. 1209–1215, 1996.
- [204] A. C. Melling, B. Ali, E. M. Scott, and D. J. Leaper, Effects of Preoperative Warming on the Incidence of Wound Infection After Clean Surgery: A Randomized Controlled Trial, *Lancet*, vol. 358, pp. 876–880, 2001.
- [205] J. M. Hynson and D. I. Sessler, Intraoperative Warming Therapies: A Comparison of Three Devices, *J. Clin. Anesth.*, vol. 4, pp. 194–199, 1992.
- [206] R. G. Oullette, Comparison of Four Intraoperative Warming Devices, *J. Am. Assoc. Nurse Anesth.*, pp. 394–396, 1993.
- [207] A. Kurz, M. Kurz, G. Poeschl, B. Faryniak, G. Redl, and W. Hackle, Forced-Air Warming Maintains Intraoperative Normothermia Better Than Circulating-Water Mattresses, *Anesth. Analg.*, vol. 77, pp. 89–95, 1993.
- [208] Murat, J. Berniere and I. Constant, Evaluation of the Efficacy of a Forced-Air Warmer (Bair Hugger) During Spinal Surgery in Children, *J. Clin. Anesth.*, vol. 6, pp. 425–429, 1994.
- [209] S. F. Borms, S. L. E. Engelen, D. G. A. Himpe, M. R. R. Suy, and W. J. H. Theunissen, Bair Hugger Forced-Air Warming Maintains Normothermia More Effectively than Thermo-Lite Insulation, *J. Clin. Anesth.*, vol. 6, pp. 303–307, 1994.
- [210] E. L. Janke, S. N. Pilkington, and D. C. Smith, Evaluation of Two Warming Systems after Cardiopulmonary Bypass, *Br. J. Anaesth.*, vol. 77, pp. 268–270, 1996.
- [211] N. Patel, C. E. Smith, D. Knapke, A. C. Pinchak, and J. F. Hagen, Heat Conservation vs. Convective Warming in Adults Undergoing Elective Surgery, *Can. J. Anaesth.*, vol. 44, pp. 669–673, 1997.



- [212] M. Berti, A. Casati, G. Torri, G. Aldegheri, D. Lungai, and G. Fanelli, Active Warming, Not Passive Heat Retention, Maintains Normothermia During Combined Epidermal-General Anesthesia for Hip and Knee Arthroplasty, *J. Clin. Anesth.*, vol. 9, pp. 483–486, 1997.
- [213] A. Kabbara, S. A. Goldlust, C. E. Smith, J. F. Hagen, and A. C. Pinchak, Randomized Prospective Comparison of Forced Air Warming Using Hospital Blankets versus Commercial Blankets in Surgical Patients, *J. Am. Soc. Anesth.*, vol. 97, pp. 338–344, 2002.
- [214] K. Wagner, E. Swanson, C. J. Raymond, and C. E. Smith, Comparison of Two Convective Warming Systems During Major Abdominal and Orthopedic Surgery, *Can. J. Anesth.*, vol. 6, pp. 358–385, 2008.
- [215] J. P. Abraham and E. M. Sparrow, Fluid Flow and Heat Transfer in Multiply-Folded, Continuous Flow Passages Including Conjugate Thermal Interaction Between the Fluid and Bounding Walls, *Numer. Heat Transfer A*, vol. 42, pp. 327–344, 2002.